

An Universal Law of the Superconducting Gap in the Electron-Doped Cuprate Superconductors

L. Shan¹, Y. Huang¹, Y. L. Wang¹, Y.Z. Zhang¹, C. Ren¹, Shiliang Li², Jun Zhao², Pengcheng Dai^{2,3}, and H. H. Wen¹
¹National Laboratory for Superconductivity, Institute of Physics & Beijing National Laboratory for Condensed Matter Physics, Chinese Academy of Sciences, P.O. Box 603, Beijing 100080, China

²Department of Physics and Astronomy, The University of Tennessee, Knoxville, Tennessee 37996-1200, USA and

³Neutron Scattering Sciences Division, Oak Ridge National Laboratory, Oak Ridge, Tennessee 37831-6393, USA

(Dated: May 26, 2019)

We use in-plane tunneling spectroscopy to study the temperature dependence of the local superconducting gap $\Delta(T)$ in electron-doped superconducting copper oxides over a wide doping range. It is found that the temperature dependence of $\Delta(T)$ follows the prediction of BCS theory for all doping levels with an universal weak coupling ratio of $\Delta(0)/k_B T_c = 1.76 \pm 0.15$. Possible reasons for this universal ratio are given and our present results strongly suggest that the electron-doped superconducting copper oxides are weak coupling BCS superconductors.

PACS numbers: 74.50.+r, 74.72.Jt, 74.45.+c

According to the Bardeen-Cooper-Schrieffer (BCS) theory of superconductivity, the superconducting gap $\Delta(T)$ is weakly temperature dependent at low temperatures but falls off rapidly to zero around T_c . In the weak coupling limit, $\Delta(0)/k_B T_c$ is 1.76 for isotropic gap and a little smaller for anisotropic gap, where $\Delta(0)$ is the zero-temperature gap averaged over the entire Fermi surface. The validity of the BCS theory in describing the high- T_c superconductivity in doped copper oxides has always been a challenging issue since their discovery. For hole-doped (*p*-type) cuprates, a ratio $\Delta_0(0)/k_B T_c = 2.14$ as expected from the *d*-wave BCS theory, where $\Delta_0(0)$ is the gap amplitude, was obtained by Angle Resolved Photo Emission Spectroscopy (ARPES) [1], quasi-particle tunneling experiments [2] and recently by the low temperature specific heat measurements in the overdoped regime[3]. However, in the underdoped regime, a pseudogap appears at the anti-nodal region and seems to compete with the superconducting gap in the same underlying Fermi surface [4, 5, 6, 7]. On the contrary, as the counterpart of the *p*-type cuprates, the electron-doped (*n*-type) ones have a much weaker or null pseudogap effect though they may be two band superconductors [8, 9, 10, 11, 12, 13, 14]. Therefore it is much easier in *n*-type cuprates to determine the superconducting gap without considering the puzzling “Fermi arc” [6, 15, 16, 17], “Nodal metal” [18, 19] or “Pseudogap”. Unfortunately, the superconducting gap of *n*-type cuprates is very small and to determine its value precisely is still a big challenge to the sensitivity and reproducibility of the current experimental methods [20, 21, 22, 23, 24, 25, 26, 27, 28]. Up to now, no any definite conclusion about the behavior of the superconducting gap has been drawn for the electron-doped system in a wide doping range.

In this Letter, we present the point contact tunneling spectroscopy data on *n*-type cuprates $Nd_{2-x}Ce_xCuO_{4-y}$ (NCCO) and $Pr_{1-x}LaCe_xCuO_{4-y}$ (PLCCO) over a wide doping range. Our data show that the temperature dependence of the average gap for all doping levels

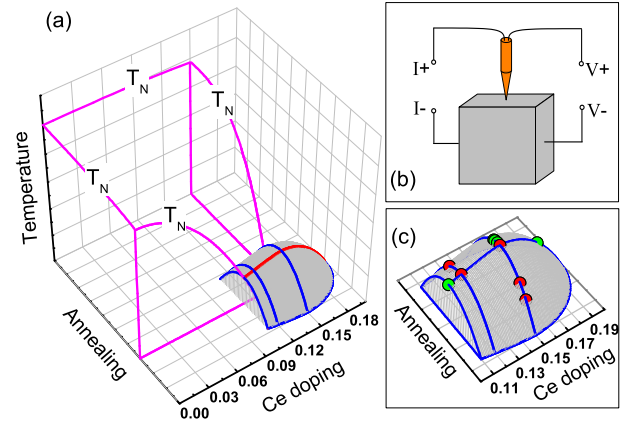


FIG. 1: (a) Electronic phase diagram of the electron-doped cuprates. The pink lines marked with T_N indicate Neel temperature. (b) The schematic diagram of the junction configuration for point-contact spectra measurements. (c) Main phases studied in this work (denoted by red dots) and that investigated by other groups using various measurements including ARPES [26, 28], Raman scattering [27], point-contact tunneling [23, 24] and grain-boundary tunneling [20].

behaves in the same way as that expected by the BCS theory. Furthermore, we show that an universal weak coupling ratio, i.e., $\Delta(0)/k_B T_c = 1.76 \pm 0.15$, is obtained for all studied *n*-type cuprate superconductors.

High-quality single crystals of NCCO and PLCCO were grown by the traveling-solvent floating-zone technique. As grown, the crystals are not superconducting. By annealing the samples of the same Ce concentration at different temperatures in pure Ar or vacuum, bulk superconductivity at different T_c 's can be obtained [29, 30, 31, 32]. Consequently, the superconducting regime in these materials is covered by a three dimensional dome in the electronic phase diagram as shown in Fig. 1(a), in which the two horizontal axes are cerium content and annealing temperature (or oxygen content)

TABLE I: Main superconducting phases studied in this work.

Label	Annealing	T_c (K)	Formula
plcco-un21	underdoped	21	$Pr_{0.88}LaCe_{0.12}CuO_{4-y}$
plcco-op24	optimally doped	24	$Pr_{0.88}LaCe_{0.12}CuO_{4-y}$
ncco-op25	optimally doped	25	$Nd_{1.85}Ce_{0.15}CuO_{4-y}$
plcco-ov17	overdoped	17	$Pr_{0.85}LaCe_{0.15}CuO_{4-y}$
plcco-ov13	overdoped	13	$Pr_{0.85}LaCe_{0.15}CuO_{4-y}$

[32], respectively. For convenience, we call the red ridge on the dome (as shown in Fig. 1(a)) as optimal doping and the higher- (lower-) oxygen portion as underdoping (overdoping). The main superconducting phases studied in this work are denoted by red dots in Fig. 1(c) and the detailed information are presented in Table I. The point-contact tunneling measurements were carried out by pointing a Pt/ Ir alloy tip or Au tip parallel to the ab -plane of the single crystals as shown in Fig. 1(b). The tip's preparation and the detailed information about the equipment were described elsewhere [33]. In order to obtain high-quality junctions with good reproducibility, the samples were carefully processed by nonaqueous chemical etching and immediately mounted on the point contact device [14]. In each superconducting phase, we repeated measurements many times at different locations on the sample surface and obtained the local information of the superconducting gap Δ and transition temperature T_c which varies slightly around the bulk values.

Fig. 2 shows the point-contact spectra measured at various doping levels. In each run of the measurement, the spectra were recorded at various temperatures between 2 K and T_c with increments of 1 K (refer to Fig. 3(a)). Only the data measured at $T = 2$ K and well above T_c are presented in Fig. 2. It can be seen clearly that all the spectra of 2 K have a similar shape with two coherence peaks and low-energy depression of the quasiparticle density of states. The peak-to-peak distance (as a rough estimate of 2Δ) increases first and then decreases with doping from underdoped to overdoped regime, which is similar to the doping dependence of T_c . The conductance within the gap voltage does not go to zero because the junctions are not tunnel junctions but ballistic point contact junctions with a finite tunneling barrier [34, 35]. For the temperature above T_c , all spectra evolve into the featureless normal-state backgrounds with similar shapes. When temperature rises crossing the superconducting transition, the junction becomes normal and the background conductance drops notably due to a finite normal-state resistance of the sample in series with the junction [36, 37]. Such conductance drop makes it difficult to distinguish the real normal-state background of the junction and has never been eliminated effectively. In this work, we remove this electrode effect simply by subtracting a constant resistance from the spectra. All spectra (above T_c) shown in Fig. 2 have been treated in this way. The good consistency of these transformed

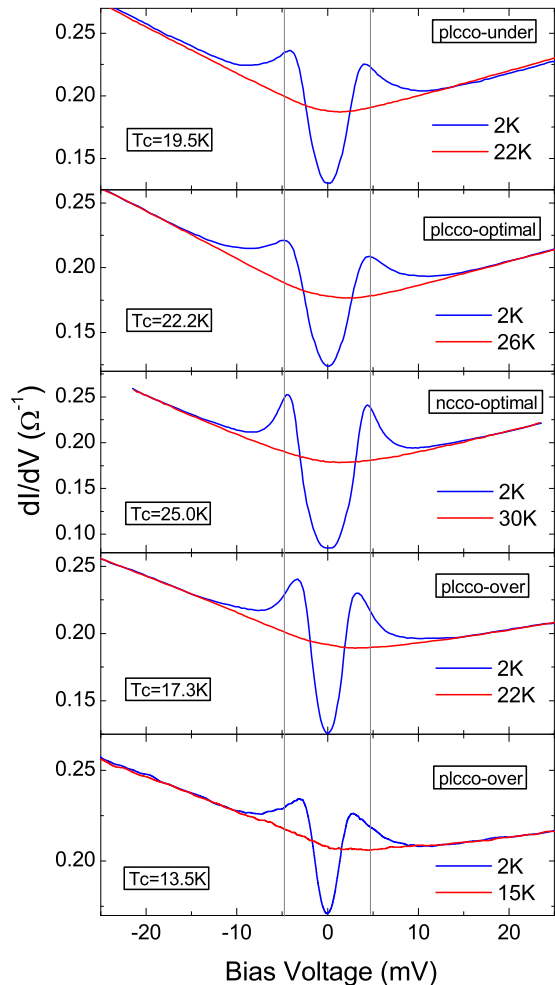


FIG. 2: Point-contact spectra measured at 2K and the temperature well above T_c for various doping levels. The conductance drop has been subtracted from the spectra above T_c as explained in the text. Two grey lines are added as references to identify the coherence peaks.

spectra with the low temperature ones at high bias voltage indicates that this simple treatment is appropriate and effective. Accordingly, we can readily construct an universal background and the spectra measured below T_c were then normalized in order to be compared with theoretical models. Here, the thermal smearing on the background was not considered because of its slight contribution.

It has been demonstrated that the basic BCS formalism, such as the energy dispersion of Bogoliubov quasiparticles, is still valid for describing the superconducting state of high T_c cuprates, although the pairing mechanism and other exotic properties may be beyond the BCS theory [38, 39]. So the noted BTK model based on the Bogoliubov equations [34] and its extended version for anisotropic superconductors [35] are still appropriate to analyze the normal-metal/superconductor (N/S) surface problems. In this model, two parameters are intro-

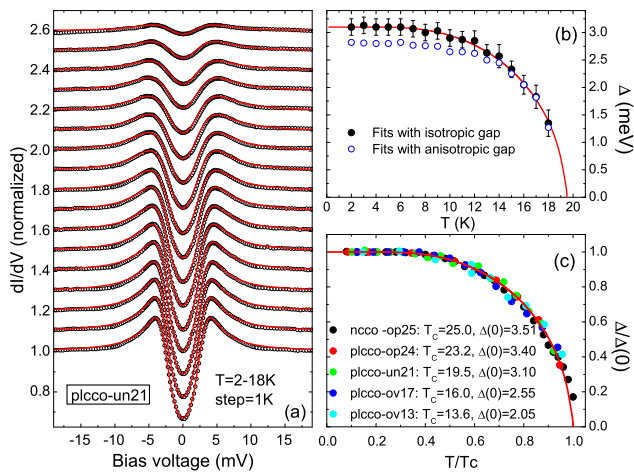


FIG. 3: (a) Temperature dependence of the normalized spectra measured on the sample plcco-un21 and theoretical calculations with the isotropic BTK model (red lines). All curves except the lowest one are shifted upwards for clarity. (b) $\Delta \sim T$ relations determined with the isotropic model (solid black circles) and the anisotropic gap model (open blue circles). Red line indicates the prediction of BCS theory. (c) Replot the temperature dependence of the superconducting gap in a reduced scale for different superconducting phases.

duced to describe the necessary physical quantities, i.e., the effective potential barrier (Z) and the superconducting energy gap (Δ). As a supplement, the quasiparticle energy E is replaced by $E + i\Gamma$, where Γ is the broadening parameter characterizing the finite lifetime of the quasiparticles [40, 41].

Fig. 3(a) shows the temperature dependence of the normalized spectra of an underdoped sample, which is in good agreement with the calculations based on the BTK model with isotropic gap (as denoted by the red solid lines). The determined gap values are presented in Fig. 3(b) as solid black circles. It is obvious that Δ is weakly temperature dependent at low temperature but falls to zero rapidly around T_c as predicted by the BCS theory (indicated by the red line in Fig. 3(b)). Remarkably, the similar $\Delta(T)$ relations were observed for all samples studied in this work [Fig. 3(c)]. We also note that all the measured spectra can be well fitted with isotropic gap while an anisotropic gap (or non-monotonic d -wave like gap) in the form of $\Delta_{anis} = \Delta_0|1.43\cos(2\phi) - 0.43\cos(6\phi)|$ has been observed for n -type cuprates [27, 28]. In order to clarify this issue, we also tried to fit the data with Δ_{anis} and a pure d -wave like gap $\Delta_d = \Delta_0|\cos(2\phi)|$ for comparison. We found that the form of Δ_{anis} is more appropriate to simulate our data than Δ_d since the Δ_d -model obviously needs a “V” shape conductance curve near zero energy which is different from the experimental data. Moreover, the Δ_{anis} -model fits the data even better than the isotropic model at higher energy outside the coherence peaks. The applicability of both the isotropic model and the anisotropic

model (Δ_{anis}) most possibly results from two reasons: 1) The inelastic scattering effect near the N/S microconstriction mentioned above (namely, there exists a finite broadening factor Γ) smears the spectra especially at the nodal region since Δ_{anis} has a sharper gap slope around the nodes and a narrower small-gap region than that of Δ_d . 2) In some cases, the nodal region has negligible contribution compared to the anti-nodal region because of the weaker spectral weight (for underdoping) [8] or fewer charge carriers (for optimal doping) [12, 14] possessed by the nodal Fermi segment. Combining these two factors, the nodal feature is difficult to be observed in the point-contact spectra. In fact, by investigating the junctions with very small broadening factors of $\Gamma < 0.2\Delta$ (built on the sample ncco-op25), we found that Δ_{anis} -model can hardly fit the spectra around zero energy unless the spectral weight of the nodal region (between $\pm 15^\circ$) is depressed. This indeed supports the picture that the contribution from the nodal Fermi segment is very limited. Therefore considering the evolution of the Fermi surface with doping and the different contributions from different segments of the Fermi surface, the effective gap function in k space should lie in the range between the constant gap (isotropic gap) model and the anisotropic model. We present in Fig. 3(b) the comparison between the constant gap obtained from the isotropic model and the average gap determined with the anisotropic model. Therefore, the real average gap have the values between these two limits and hence can be determined accurately.

Based on Fig. 3, we can obtain not only the temperature dependence of the average gap but also the corresponding T_c by extrapolating the $\Delta(T)$ curve to the horizontal axis. The local T_c at the given location on the sample surface determined in this way varies slightly (below $\pm 1.5K$) around the bulk value determined by the magnetization measurement. The obtained $\Delta(0)$ and T_c (by fitting to the isotropic model) at various locations on different samples are presented in Fig. 4. For comparison, in Fig. 4 we also accumulate the data given in previous reports (green symbols) [20, 23, 24, 26, 27, 28], corresponding to the doping levels indicated by green dots shown in Fig. 1(c). The coupling ratio is almost constant with a value around 1.76. If the anisotropic gap function is used, this ratio becomes about 1.6 (as indicated by the black spheres). In order to demonstrate the validity of the methodology for determining the superconducting gap, we have also measured the point-contact spectra of Nb-tip/Au-foil using the same experimental apparatus. The determined coupling ratio is in good agreement with previous reports [42] and the BCS theory, as shown in Fig. 4 by the filled up triangles. The results suggest that the n -type cuprates are weak coupling BCS superconductors although the pairing symmetry may not be of s-wave since the ratio 1.76 can also be obtained if the Fermi segment near the nodal region has negligible contributions to the tunneling signal either by the quasiparticle lifetime broadening or naturally it is small. However, it should be pointed that one of the n -type

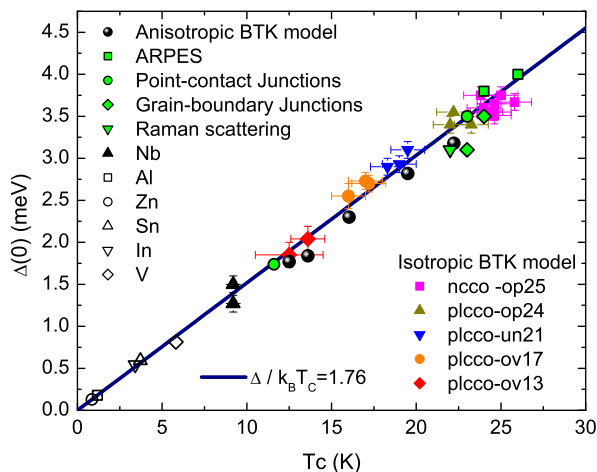


FIG. 4: Relationship between the zero-temperature average gap and transition temperature. The green symbols indicate previous reports from different measurements including ARPES [26, 28], Raman scattering [27], point-contact tunneling [23, 24] and grain-boundary tunneling [20], corresponding to the doping levels marked by green dots in Fig. 1(c). The black spheres indicate the results of fitting to the anisotropic model. The solid black up-triangles indicate the parameters of Nb measured by the same experimental apparatus used in this work. The data of some conventional superconductors are also presented as open symbols for comparison [42].

cuprates $Sr_{0.9}La_{0.1}CO_2$ may be an exception since it is an infinite-layer cuprate superconductor and has a quite

large coupling ratio $\Delta(0)/k_B T_c \approx 3.5$ [43], which is an interesting issue to be addressed in the future.

In summary, by investigating the point-contact tunneling spectra of the electron doped cuprates with various doping levels, we show that the temperature dependence of the superconducting gap follows the BCS prediction very well for samples in wide doping regime and obeys an universal law with a weak coupling ratio $\Delta(0)/k_B T_c = 1.76 \pm 0.15$. Therefore, the electron doped cuprates are weak coupling BCS superconductors.

Note added: During the preparation of this manuscript, we became aware that a recent report indicates the weak coupling BCS dirty superconductivity in an electron doped cuprate based on the measurements of SIS' junctions[44].

Acknowledgments

This work is supported by the National Science Foundation of China, the Ministry of Science and Technology of China (973 project No: 2006CB601000, 2006CB921802), and Chinese Academy of Sciences (Project ITSNEM). The PLCCO and NCCO single-crystal growth at UT is supported by the US DOE BES under contract No. DE-FG-02-05ER46202. We acknowledge the fruitful discussions with Zhi-Xun Shen and N. Nagaosa.

E-mail address: shanlei@ssc.iphy.ac.cn (L. Shan); hhwen@aphy.iphy.ac.cn (H. H. Wen)

-
- [1] A. Ino *et al.*, Phys. Rev. B **65**, 094504 (2002).
[2] T. Nakano *et al.*, J.Phys.Soc.Japan **67**, 2622 (1998).
[3] Yue Wang *et al.*, unpublished.
[4] T. Yoshida *et al.*, cond-mat/0510608 (2005).
[5] A. Damascelli, Z. Hussain, and Z.X. Shen, Rev. Mod. Phys. **75**, 473(2005) and references therein.
[6] H.H. Wen *et al.*, Phys. Rev. B **72**, 134507 (2005).
[7] A. D. Beyer, C.-T. Chen, and N.-C. Yeh, cond-mat/0610855 (2006).
[8] N. P. Armitage *et al.*, Phys. Rev. Lett. **88**, 257001 (2002).
[9] H. Matsui *et al.*, Phys. Rev. Lett. **94**, 047005 (2005).
[10] Q. S. Yuan *et al.*, Phys. Rev. B **69**, 214523 (2004).
[11] C. Kusko *et al.*, Phys. Rev. B **66**, 140513(R) (2002).
[12] H. G. Luo and T. Xiang, Phys. Rev. Lett. **94**, 027001 (2005).
[13] C. S. Liu *et al.*, Phys. Rev. B **73**, 174517 (2006).
[14] L. Shan *et al.*, Phys. Rev. B **72**, 144506 (2005).
[15] M. R. Norman, D. Pines and C. Kallin, Advances in Physics, **54**, 715 (2005).
[16] K. Tanaka *et al.*, cond-mat/0612048 (2006).
[17] M. Hashimoto *et al.*, cond-mat/0610758 (2006).
[18] T. Valla *et al.*, Science **314**, 1914 (2006).
[19] A. Kanigel *et al.*, Nature Physics **2**, 447 (2006).
[20] S. Kleefisch *et al.*, Phys. Rev. B **63**, 100507(R) (2001).
[21] S. Kashiwaya *et al.*, Phys. Rev. B **57**, 8680 (1998).
[22] A. Mourachkine, Europhys. Lett. **50**, 663 (2000).
[23] Q. Huang *et al.*, Nature **347**, 369 (1990).
[24] Amlan Biswas *et al.*, Phys. Rev. Lett. **88**, 207004 (2002).
[25] M. M. Qazilbash *et al.*, Phys. Rev. B **68**, 024502 (2003).
[26] N. P. Armitage *et al.*, Phys. Rev. Lett. **86**, 1126 (2001).
[27] G. Blumberg *et al.*, Phys. Rev. Lett. **88**, 107002 (2002).
[28] H. Matsui *et al.*, Phys. Rev. Lett. **95**, 017003 (2005).
[29] Pengcheng Dai *et al.*, Phys. Rev. B **71**, 100502 (2005).
[30] Y. Tokura, H. Takagi and S. Uchida, Nature **337**, 345 (1989).
[31] H. Takagi, S. Uchida and Y. Tokura, Phys. Rev. Lett. **62**, 1197 (1989).
[32] H. J. Kang *et al.*, Nature Mater. **6**, 224 (2007).
[33] L. Shan *et al.*, Phys. Rev. B **68**, 144510 (2003).
[34] G.E. Blonder, M. Tinkham, and T.M. Klapwijk, Phys. Rev. B **25**, 4515 (1982).
[35] Y. Tanaka and S. Kashiwaya, Phys. Rev. Lett. **74**, 3451 (1995); Phys. Rev. B **53**, 9371 (1996).
[36] L. Alff *et al.*, Nature **422**, 698 (2003).
[37] Amlan Biswas *et al.*, Phys. Rev. B **64**, 104519 (2001).
[38] H. Matsui *et al.*, Phys. Rev. Lett. **90**, 217002 (2003).
[39] J. E. Hoffman *et al.*, Science **297**, 1148 (2002).
[40] R. C. Dynes *et al.*, Phys. Rev. Lett. **53**, 2437 (1984).
[41] A. Plecenfk *et al.*, Phys. Rev. B **49**, 10016 (1994).
[42] E. L. Wolf, *Principles of Electron Tunneling Spectroscopy*. (Oxford Univ. Press, New York, 1985).
[43] C.-T. Chen *et al.*, Phys. Rev. Lett. **88**, 227002 (2002).

[44] Y. Dagan, R. Bek, R. L. Greene, *Condmat*/0702091.